Published in final edited form as:
J Neurochem. 2010 January 1; 112(1): 173. doi:10.1111/j.1471-4159.2009.06438.x.

Protein aggregationin neurons following OGD: a role for Na^+ and Ca^{2+} ionic dysregulation

Xinzhi Chen[1,2], **Douglas B. Kintner**[2], **Akemichi Baba**[3], **Toshio Matsuda**[3], **Gary E. Shull**[4], and **Dandan Sun**[1,2]

[1] Neuroscience Training Program, Univ. of Wisconsin School of Medicine and Public Health, Madison, Waisman Center, WI 53705

[2] Dept. of Neurological Surgery, Univ. of Wisconsin School of Medicine and Public Health, Madison, Waisman Center, WI 53705

[3] Graduate School of Pharmaceutical Sciences, Osaka University, Osaka, Japan

[4] Dept. of Molecular Genetics, Biochem. and Microbiology, Univ. of Cincinnati, Cincinnati, OH 45267

Abstract

In this study, we investigated whether disruption of Na^+ and Ca^{2+} homeostasis via activation of Na^+-K^+-Cl^- cotransporter (NKCC1) and reversal of Na^+/Ca^{2+} exchange (NCX_{rev}) affects protein aggregation and degradation following oxygen-glucose deprivation (OGD). Cultured cortical neurons were subjected to 2 h OGD and 1–24 h reoxygenation (REOX). Redistribution of ubiquitin and formation of ubiquitin-conjugated protein aggregates occurred in neurons as early as 2 h REOX. The protein aggregation progressed further by 8 h REOX. There was no significant recovery at 24 h REOX. Moreover, the proteasome activity in neurons was inhibited by 80–90% during 2–8 h REOX and recovered partially at 24 h REOX. Interestingly, pharmacological inhibition or genetic ablation of NKCC1 activity significantly decreased accumulation of ubiquitin-conjugated protein aggregates and improved proteasome activity. A similar protective effect was obtained by blocking NCX_{rev} activity. Inhibition of NKCC1 activity also preserved intracellular ATP and Na^+ homeostasis during 0–24 h REOX. In a positive control study, disruption of endoplasmic reticulum Ca^{2+} with thapsigargin triggered redistribution of free ubiquitin and protein aggregation. We conclude that overstimulation of NKCC1 and NCX_{rev} following OGD/REOX partially contributes to protein aggregation and proteasome dysfunction as a result of ionic dysregulation.

Keywords

oxygen and glucose deprivation; ischemia-reperfusion; unfolded protein response; bumetanide; protein aggregation; proteasome activity

INTRODUCTION

Abnormal protein aggregates are detected in brains under several neurodegenerative disease conditions including cerebral ischemia (Kakizuka 1998). Protein ubiquitination and degradation of ubiquitin-conjugated proteins (ubi-proteins) by proteasome activity are ATP-dependent (Eytan et al. 1989; Benaroudj et al. 2003). Cerebral ischemia with reduced level of

Address correspondence to: Dandan Sun, M.D., Ph.D., Department of Neurological Surgery, University of Wisconsin Medical School, T513 Waisman Center, 1500 Highland Ave., Madison, WI 53705, Phone: (608) 263-4060, FAX: (608) 263-1409, sun@neurosurg.wisc.edu.

ATP may impair chaperone function, ubiquitin-proteasomal degradation, and lead to protein aggregation (DeGracia and Hu 2007). Depletion of free ubiquitin occurs in CA1 neurons during 3–48 h reperfusion following transient forebrain ischemia (Ide et al. 1999). A sustained decrease in 26S proteasome activity in CA1 neurons is detected during 30 min–48 h reperfusion (Asai et al. 2002). Ischemia-reperfusion causes accumulation of high molecular weight ubi-proteins following forebrain ischemia (Hu et al. 2001). These ubiquitinated-protein aggregates are clustered with subcellular structures (Hu et al. 2000; Hu et al. 2001), chaperones, protein folding enzymes (Liu et al. 2005), proteasomes (Ge et al. 2007), and stress granules (DeGracia et al. 2007). These changes may contribute to sustained translation arrest and ischemic neuronal damage.

Dysregulation of endoplasmic reticulum Ca^{2+} (Ca^{2+}_{ER}) can disrupt proper peptide folding and trigger the unfolded protein response and ER stress (Groenendyk and Michalak 2005; Paschen and Doutheil 1999). Maturation and folding of membraneand secretory proteins rely on the activity of Ca^{2+}-regulated ERchaperones and enzymes. Depletion of Ca^{2+}_{ER} will perturb the function of these proteins and result in formation of misfolded proteins which are subsequently degraded by the ubiquitin-proteasomal system (Groenendyk and Michalak 2005). Therefore, maintenance of Ca^{2+}_{ER} homeostasis is important for appropriate protein folding.

Na^+-K^+-Cl^- cotransporter isoform 1 (NKCC1) transports Na^+, K^+, and Cl^- in cells under physiological conditions (Russell 2000). Our recent study demonstrates that NKCC1 in conjunction with reversed mode operation of Na^+/Ca^{2+} exchanger (NCX_{rev}) plays a role in Na^+ and Ca^{2+}overload and disruption of Ca^{2+}_{ER} homeostasis in neurons following oxygen-glucose deprivation (OGD) and reoxygenation (REOX) (Chen et al. 2008). Inhibition of NKCC1 activity with its inhibitor bumetanide (Bu) or genetic ablation prevents the release of Ca^{2+}_{ER} and ER stress development (Chen et al. 2008). In the present study, we examined whether formation of ubi-proteins occurs in neurons following OGD/REOX and whether inhibition of NKCC1 and NCX_{rev} decreases accumulation of ubi-proteins. We report here that a time-dependent formation of ubiquitin-protein aggregates was detected in neurons during 2–24 h REOX after 2 h OGD, which was accompanied by decreased proteasome activity. Blocking NKCC1 activity significantly attenuated formation of ubi-proteins and preserved proteasome function following *in vitro* ischemia.

MATERIALS AND METHODS

Materials

Hanks balanced salt solution (HBSS) was from Mediatech Cellgro (Manassas, VA). Neurobasal medium, B-27 supplement, fura-2 AM, furaptra-AM (mag-fura-2-AM), sodium-binding benzofuran isophthalate (SBFI-AM), 4-bromo A-23187, Alexa Fluor 488 goat anti-mouse IgG, and To-pro-3 iodide were from Invitrogen (Carlsbad, CA). Pluronic acid was purchased from BASF (Ludwigshafen, Germany). Bumetanide, gramicidin, monensin and thapsigargin were from Sigma (St. Louis, MO). SEA0400 was a kind gift from Taisho Pharmaceutical CO. Ltd. (Omiya, Saitama, Japan). The monoclonal antibody against ubiquitin for Western blotting was from Chemicon (Temecula, CA). The monoclonal anti-ubiquitin antibody for immunostaining was from Novus Biologicals (Littleton, CO). ATP assay kit was from PerkinElmer Life and Analytical Sciences (Waltham, MA). The Proteasome-Glo Cell-Based assay kit was from Promega Bioscience (Madison, WI).

Pure cortical neuronal cultures

Embryonic day 14–16 pregnant mice (SV129/Black Swiss) were anesthetized with 5% halothane (Beck et al. 2003). Fetuses were removed and the cortices dissected in ice-cold HBSS. The tissues were treated with 0.5 mg/ml trypsin at 37°C for 25 min. The cells were

centrifuged at 350 g at 4°C for 4 min. The cell suspension was diluted in B-27 supplemented Neurobasal medium (2%) containing 0.5 mM L-glutamine and penicillin/streptomycin (100 units/ml and 0.1 mg/ml, respectively). The cells (200–1000 cells/mm^2) were seeded in plates or on glass coverslips coated with poly-D-lysine. Cultures were incubated at 37°C in an incubator with 5% CO_2 and atmospheric air and re-fed with fresh medium every 3 days. Cultures at 10–12 days *in vitro* (DIV) were used in the study.

To obtain NKCC1$^{-/-}$ neuron cultures, male and female gene-targeted NKCC1 heterozygous mutant mice were bred as described before (Flagella et al. 1999). NKCC1$^{+/+}$ and NKCC1$^{-/-}$ cultures were established from the E14–16 fetuses. The genotype of each fetus was determined by a polymerase chain reaction of DNA from fetus tail biopsies. Experiments were performed in parallel in NKCC1$^{+/+}$ and NKCC1$^{-/-}$ cultures obtained from littermates.

OGD treatment

DIV 10–12 neuronal cultures were rinsed with an isotonic OGD solution (pH 7.4) containing (in mM): 0 glucose, 20 $NaHCO_3$, 120 NaCl, 5.36 KCl, 0.33 Na_2HPO_4, 0.44 KH_2PO4, 1.27 $CaCl_2$, 0.81 $MgSO_4$, as described before (Lenart et al. 2004). K^+ concentration (~ 5.8 mM) was used in the OGD solution which is similar to the Neurobasal medium (5.4 mM K^+). The cells were incubated in the OGD solution for 2 h in a hypoxic incubator (model 3130, Thermo Forma, Marietta, OH) containing 94% N_2, 1% O_2, and 5% CO_2. The oxygen level in the OGD solution decreased to ~2–3% after 60 min in the hypoxic incubator (Beck et al. 2003). Normoxic control cells were incubated for 2 h in 5% CO_2 and atmospheric air in a normoxic buffer identical to the OGD solution except containing 5.5 mM glucose. Reoxygenation was achieved by incubating cells with equal volume of Neurobasal medium containing 5.5 mM glucose at 37°C in 5% CO_2 and atmospheric air. For 15 min–2 h REOX experiments, cultures were incubated in the normoxic buffer in the incubator at 37°C in 5% CO_2 and atmospheric air.

Preparation of detergent/salt insoluble protein aggregate-containing fractions

Triton X-100 (TX)/KCl insoluble protein aggregate fraction was prepared as described by Hu et al (Hu et al. 2001). Cultured neurons were washed with ice-cold PBS and sonicated for 30 sec at 4°C in ice-cold lysis buffer (pH 7.6) containing (mM): 15 Tris base/HCl, 1 dithiothreitol, 250 sucrose, 1 $MgCl_2$, 2.5 EDTA, 1 EGTA, 250 Na_3VO_4, 25 NaF, 0.2 sodium pyrophosphate, 0.5 phenylmethylsulfonyl fluoride, plus 1 μg/mL pepstatin A, 5 μg/mL leupeptin, and 2.5 μg/mL aproptonin. Protein content in lysates was determined by the bicinchoninic acid (BCA) method (Pierce, Rockford, IL). Equal amount of total cell lysate protein in each sample (0.5 mg) was centrifuged at 12,000 g at 4°C for 10 min. The pellet fractions were sonicated 3 times (each for 5 sec.) and washed for 1 h at 4°C with 2% TX and 150 mM KCl in the ice-cold lysis buffer. The samples were centrifuged at 12,000 g at 4°C for 10 min. The pellet fraction containing the TX-insoluble aggregates was sonicated and re-dissolved in the lysis buffer without TX/KCl for Western blotting assay.

Gel electrophoresis and Western blotting

TX-insoluble protein aggregate fractions were denatured electrophoretically separate by 10% sodium dodecyl sulfate-polyacrylamide gel electrophoresis (SDS-PAGE). Each TX-insoluble pellet was loaded in a single gel lane. The resolved proteins were electrophoretically transferred to a PVDF membrane. The blots were incubated in 7.5% nonfat dry milk in tris-buffered saline (TBS) overnight at 4°C and then incubated for 1 h with a primary monoclonal antibody against ubiquitin (1:1000). The blots were rinsed with TBS and incubated with horseradish peroxidase-conjugated secondary IgG for 1 h. Bound antibody was visualized using an enhanced chemiluminescence assay (Amersham Corp, Piscataway, NJ). Membranes were scanned and average pixel intensity of the high-molecular-weight area (protein smear range between 37–

250 kDa) in each lane quantified using ImageJ software (ImageJ, National Institutes of Health, Bethesda, MD).

Immunofluorescence staining of ubiquitin

Neurons on coverslips were fixed with 4% paraformaldehyde in PBS for 20 min. After rinsing, cells were incubated with the blocking solution (10% normal goat serum, 0.4% TX, and 1% bovine serum albumin in PBS) for 30 min followed by incubation at room temperature with the anti-ubiquitin monoclonal antibody (1:200). After rinsing in PBS, coverslips were incubated with Alexa Fluor 488 anti-mouse IgG (1:200) for 1 h at 37°C. After rinsing with PBS, To-pro-3 iodide (1 μg/mL in PBS) was added to stain nuclei and the coverslips were mounted on the slide. Confocal images (512 × 512 pixels, 200 Hz) were acquired sequentially with a Leica DMIRE2 microscope (Exton, PA) using a 63× 1.4 NA apochrome objective. An argon laser was used for Alexa Fluor 488, and a 640 nm GreNe laser for To-pro-3 iodide signals. Image stacks were acquired at 0.1 μm intervals for 20 optical sections and an orthographic projection of average intensity applied. Some of images were magnified for illustration.

26S proteasome activity assay

Proteasome-Glo cell-based assay was used to determine proteasomal activity with N-succinyl-Leu-Leu-Val-Tyr-aminoluciferin as a substrate (Promega, Madison, WI), which reflects the chymotrypsin-like activity of the 26S. In brief, culture medium in each well of 24-well plates was replaced with 400 μl normoxic buffer and incubated at room temperature for 10 min. Proteasome-Glo Substrate (0.2 μM) in lysis buffer was added into each well and the plates were incubated at room temperature for another 30 min. 200 μl reaction sample was taken for determination of luminescence with an Lmax II Luminometer (Molecular Devices, Sunnyvale, CA). 20 μl reaction sample was taken for determination of protein content by the BCA method. Proteasomal activity in each sample was expressed as relative light units (RLU) per milligram protein.

Measurement of intracellular ATP content

Intracellular ATP content was measured using a luminescence ATP detection assay according to the manufacturer's instructions (PerkinElmer, Boston, MA). At the end of each experiment, culture medium in each well of 24-well plates was replaced with 250 μl normoxic buffer. Lysis solution (125 μl) was added into each well, and plates were gently swirled for 5 min. 125 μl substrate was added into each cell lysate and plates were gently swirled for 5 min and incubated in dark for 10 min. Protein content in cell lysates was determined by the BCA method. Luminescence in each sample and ATP standards was detected with an Lmax II Luminometer. Intracellular ATP content was expressed as nanomoles per milligram protein.

Intracellular Na^+ measurement—Intracellular Na^+ concentration ($[Na^+]_i$) was measured with the fluorescent dye SBFI-AM as described previously with some modifications (Lenart et al. 2004). Cultured neurons grown on coverslips were loaded with 15 μM SBFI-AM plus 0.02% pluronic acid during 2 h OGD or during the last 2 h of REOX. For 1 and 2 h REOX, 5.5 mM glucose was added to the OGD solution and coverslips were placed in a normoxic incubator at 37°C in 5% CO_2 and atmospheric air. For 24 h REOX, OGD solution was replaced with Neurobasal medium and incubated at 37°C in 5% CO_2 and atmospheric air for 22 h. At the end of REOX, coverslips were placed in a open-bath imaging chamber and superfused (1 ml/min) with HCO_3^--MEM at 37°C. Using the Nikon TE 300 inverted epifluorescence microscope and a 40X lens, neurons were excited at 345 nm and 385 nm and the emission fluorescence at 510 nm recorded every 20 sec for 2 min. The 345/385 ratios were analyzed with the MetaFluor image-processing software. Absolute $[Na^+]_i$ was determined for each cell

by performing an in-situ calibration at the end of each experiment as described before (Lenart et al. 2004).

Ca^{2+}_{ER} measurement—Ca^{2+}_{ER} was determined in normoxic neurons, or neurons subjected to 0, 15 min, 1, 2, or 24 h REOX. Coverslips were incubated with 4 μM mag-fura-2 AM and 0.02 % pluronic acid as for two hours as previously described (Chen et al. 2008). For the 0, 15 min and 1 h REOX, the cells were incubated with the dye during OGD. The cells were loaded during the last 2 h of REOX for 2 and 24 h REOX experiments. After loading, the coverslips were quickly (< 2 min) placed on the open-bath imaging chamber in HEPES-MEM at 37°C. Cells were excited every 10 sec at 345 and 385 nm and the emission fluorescence images collected at 510 nm using Nikon TE 300 inverted epifluorescence microscope and a 40X objective lens. To determine Ca^{2+}_{ER}, the plasma membrane was permeablized with 30 sec exposure to saponin (30.0 μg/ml) in an intracellular solution to eliminate the cytosolic mag-fura-2 signal as previously described (Chen et al. 2008). The mag-fura-2 signal in ER was calibrated in each experiment and Ca^{2+}_{ER} calculated using a K_a of 56 μM that was determined in neurons using solutions of known Ca^{2+} concentrations as described before (Chen et al. 2008). Ca^{2+}_{ER} was determined in normoxic neurons, or neurons subjected to 0, 15 min, 1, 2, or 24 h REOX.

Statistics—Statistical significance was determined by student's t-test or an ANOVA in the case of multiple comparisons. A P-value smaller than 0.05 was considered statistically significant. N values represent the number of cultures used in each experiment.

RESULTS

OGD/REOX triggers formation of TX-insoluble protein aggregates

The majority of known protein substrates of proteasomes must be polyubiquitinated prior to proteolysis (Haas and Rose 1982). Protein aggregates have lower solubility in detergent TX/KCl solution (Hu et al. 2001). Therefore, in the current study, formation of TX-insoluble ubi-protein aggregates was examined in neurons under normoxic control conditions or after exposure to 2 h OGD and 2–24 h REOX. Under normoxic control conditions, little ubi-proteins were detected in neurons. This is similar to the findings in *in vivo* sham control studies (Ge et al. 2007). In contrast, during 2–24 h REOX, there was a time-dependent accumulation of ubi-proteins (> 37 kDa, illustrated with the classical ubiquintinated smear in the 37–250 kDa range in Figure 1A). 2 h REOX led to an ~ 2.2-fold increase in formation of ubi-proteins ($p < 0.05$, Figure 1A, B). The level of protein aggregation was further developed over 2 – 8 h REOX reaching ~ 9-fold at 8 h REOX. If using area density analysis (instead of average pixel intensity), 8 h REOX led to an ~ 30-fold increase in Ubi-proteins. Ubi-proteins remained significantly elevated at 24 h REOX (Figure 1B). These results suggest that OGD/REOX causes a progressive ubiquitination of misfolded proteins and aggregate formation in neurons which lasts at least 24 h.

We reported recently that inhibition of NKCC1 prevents depletion of Ca^{2+}_{ER} and reduces ER stress (Chen et al. 2008). Therefore, we hypothesized that blocking NKCC1 may subsequently decrease misfolded protein formation. As shown in Figure 1A, B, we examined changes of ubi-protein levels in neurons when NKCC1 is inhibited with the potent inhibitor Bu. In the presence of Bu (10 μM), at 2, 4, 8, 24 h REOX, the levels of ubi-proteins were significantly lower than the non-treated controls ($p < 0.05$). A similar protective result was observed in $NKCC1^{-/-}$ neurons when exposed to 2 h OGD and 4 h REOX (Figure 1C, D).

We hypothesized that the protective effects via NKCC1 inhibition in part results from preserving Ca^{2+}_{ER} homeostasis. The hypothesis was tested by two control experiments. First, we investigated whether blocking Sarco/Endoplasmic Reticulum Ca^{2+} ATPase (SERCA) with

thapsigargin (Tg) triggers protein misfolding and increases ubi-proteins. As shown in Figure 1E, inhibition of SERCA with Tg (0.1 μM) for 24 h led to ~ 2.8-fold increase in ubi-proteins. This indicates that disruption of Ca^{2+}_{ER} can cause protein misfolding and accumulation of ubi-proteins. In the present study, 100 nM thapsigargin was used because 1 μM thapsigargin caused 90% cell death in cultured pure neurons after 24 h even though 1 μM thapsigargin is commonly used in neuron-glia mixed cultures. Moreover, because NCX_{rev} is stimulated following NKCC1-mediated Na^+ overload and contributes to Ca^{2+}_{ER} dysregulation, we speculate that pharmacological inhibition of NCX_{rev} would be able to attenuate the formation of ubi-proteins. Blocking NCX_{rev} by its potent inhibitor SEA0400 (1 μM) reduced the ubi-protein formation by ~ 50% at 4 h REOX, compared to the 4 h REOX control group (Figure 1E, F). These data further support our view that activation of NKCC1/NCX_{rev} plays a role in formation of ubi-proteins following OGD/REOX.

OGD/REOX-induced ubiquitin re-distribution and formation of ubi-proteins

A monoclonal anti-ubiquitin antibody recognizing both free and conjugated ubiquitin was used to monitor ubiquitin re-distribution and formation of ubi-proteins. In normoxic control neurons, the ubiquitin immunoreactivity was diffuse and evenly distributed in soma and processes (Figure 2A, arrow). In $NKCC1^{+/+}$ neurons subjected to 2 h OGD/4 h REOX, the diffuse distribution of free ubiquitin was absent in most cells. Instead, the ubiquitin immunoreactivity was clustered near nuclei (Figure 2B, arrowhead). This change was further illustrated in the magnified images (Figure 2C, D). Interestingly, inhibition of NKCC1 with its inhibitor Bu prevented the ubiquitin re-distribution after OGD/REOX (Figure 2E), with the majority of neurons showing diffuse ubiquitin staining pattern similar to normoxic controls. Genetic ablation of NKCC1 had similar protective effects in $NKCC1^{-/-}$ neurons (Figure 2F). Moreover, inhibition of NCX_{rev} with SEA0400 (1 μM) during REOX significantly attenuated the OGD/REOX-induced ubiquitin re-distribution (Figure 2G, I). In a positive control study with the SERCA inhibitor Tg, ubi-proteins clustered near nuclei in a similar fashion as in OGD/REOX-treated neurons (Figure 2H). Summarized data of the percentage of neurons with ubi-proteins were shown in Figure 2I. ~ 35% of neurons exhibited punctuate ubiquitin staining in the peri-nucleus regions at 4 h REOX ($p < 0.05$). In contrast, either inhibition of NKCC1 or NCX_{rev} significantly attenuated the OGD/REOX-mediated changes in ubiquitin re-distribution. Depletion of Ca^{2+}_{ER} with Tg triggered an ~ 40% increase in formation of ubi-proteins. These results further establish that OGD/REOX causes an increase in ubi-conjugated protein formation and inhibition of NKCC1/NCX_{rev} attenuates the process.

Inhibition of NKCC1 activity attenuates Ca^{2+}_{ER} dysregulation and promotes proteasomal activity after OGD/REOX

Ca^{2+}_{ER} in normoxic control neurons was 8.5 ± 1 μM (Figure 3A). 2 h OGD resulted in increased Ca^{2+} loading into ER (~2.3 fold) followed by a transient depletion of Ca^{2+}_{ER} at 15 min REOX, which is similar to our previous report (Chen et al. 2008). Ca^{2+}_{ER} stores refilled by 1 h REOX and remained elevated for 24 h (Figure 3A). Moreover, inhibition of NKCC1 activity with Bu prevented Ca^{2+}_{ER} depletion. In a positive control experiment, exposure of neurons to the SERCA inhibitor Tg (0.1 μM for 24 h) triggered 85% release of Ca^{2+}_{ER}. The data suggest that inhibition of NKCC1 reduces Ca^{2+}_{ER} release which may preserve ER protein folding function.

Reduction of proteasomal activity following OGD/REOX may also contribute to elevation of misfolded protein and accumulation of ubi-proteins. Thus, we investigated changes of proteasomal activity of the 26S in neurons under normoxic control or 2–24 h REOX conditions. As shown in Figure 3B, 26S proteasomal activity was 240 ± 30 RLU/mg protein in normoxic control neurons. Neurons exposed to 2 h OGD and 2 h REOX exhibited a low level of 26S proteasomal activity (43 ± 4 RLU/mg protein). 26S proteasomal activity remained inhibited (~ 80–90%) during 4–8 h REOX. At 24 h, 26S proteasomal activity recovered by ~ 60 % ($p <$

0.05**,** Figure 3B). Interestingly, the decline of 26S proteasomal activity at 2 h REOX was absent when NKCC1 was pharmacologically inhibited. Moreover, in the presence of Bu, 26S proteasomal activity was partially restored (30–40%) at 4–8 h REOX. At 24 h REOX, neurons treated with Bu had a level of 26S proteasomal activity similar to normoxic neurons (Figure 3B). Interestingly, NKCC1$^{-/-}$ neurons showed little inhibition of 26S proteasomal activity following OGD/REOX (Figure 3C). Moreover, blocking NCX_{rev} by SEA0400 prevented the OGD/REOX-mediated inhibition of 26S proteasomal activity (Figure 3C). These results indicate that OGD/REOX persistently inhibits proteasomal activity, which may lead to formation of ubi-proteins in neurons. In contrast, decrease of ionic homeostasis dysregulation by blocking NKCC1/NCX_{rev} activity preserves the proteasomal activity.

Inhibition of NKCC1 activity preserves intracellular ATP level and Na^+ homeostasis following OGD/REOX

OGD/REOX-mediated inhibition of proteasomal activity may result from reduction of intracellular ATP levels. To test this possibility, we measured intracellular ATP content in normoxic neurons or neurons subjected to 0–24 h REOX following 2h OGD. Figure 4A shows that ATP was 11 ± 1 nmol/mg protein in normoxic control neurons. At 0 h REOX, the ATP level fell to ~12% of normoxic control. The ATP content remained at 20% of control during 1–2 h REOX. Surprisingly, no significant recovery was detected at 24 h REOX. Pharmacological inhibition of NKCC1 maintained ATP levels at 30–40 % during 0–24 h REOX. Consistent with this finding, NKCC1$^{-/-}$ neurons exhibited significantly higher ATP levels (~ 40% of control) at 0, 1, 2 h REOX. Intracellular ATP level in NKCC1$^{-/-}$ neurons completely recovered at 24 h REOX (Figure 4A). These results indicate that inhibition of NKCC1 activity preserves intracellular ATP content following OGD/REOX.

We speculated that blocking NKCC1 can preserve intracellular ATP content in part because it reduces NKCC1-mediated Na^+ entry and ATP-dependent Na^+ efflux via Na^+/K^+-ATPase. Thus, we determined changes of $[Na^+]_i$ following OGD/REOX. 2 h OGD caused an increase in $[Na^+]_i$ from 13.1 ± 0.5 mM to 24.3 ± 1.3 mM ($p < 0.05$, Figure 4B). $[Na^+]_i$ further rose to ~ 43 mM at 1 –2 h REOX and returned to 17.3 ± 3.0 mM at 24 h REOX which was not significantly different from the basal levels. Inhibition of NKCC1 activity with Bu reduced $[Na^+]_i$ by 20–50% during 0–2 h REOX (Figure 4B, $p < 0.05$). Moreover, blocking NKCC1 activity also resulted in a significant decrease in baseline $[Na^+]_i$ (13.1 vs. 9.5 mM, $p < 0.05$) which suggests a role for NKCC1 in resting level of $[Na^+]_i$. Taken together, these data imply that Na^+/K^+-ATPase alone cannot maintain Na^+_i homeostasis when NKCC1 activity is overstimulated following OGD/REOX.

DISCUSSION

Formation of protein aggregates in cortical neurons following OGD/REOX

Transient cerebral ischemia induces irreversible misfolded protein aggregate formation. In a two-vessel transient occlusion model of global ischemia, CA1 neurons exhibit a patchy pattern of ubi-protein expression around nuclei and along dendritic membranes during 4–24 h reperfusion after 15 min ischemia (Hu et al. 2000). Ubiquitin-immunogold labeled protein aggregates were detected in CA1 neurons after ischemia and their number increased further by 24 h reperfusion (Hu et al. 2000). A similar result was observed at 1, 4, and 24 h reperfusion after 2 h middle cerebral artery occlusion (Hu et al. 2001). The ubi-positive immunoclusters are misfolded/damaged protein aggregates clumped with the ER, mitochondria, nuclei, and cell membranes (Hu et al. 2000). In addition, chaperones and protein folding enzymes, as well as, proteosomes are sequestered in these protein aggregates in post-ischemic brains (Liu et al. 2005; Ge et al. 2007; Zhang et al. 2006). Recently, it has been reported that ubi-containing aggregates and stress granules were converged in CA1 neurons at 2–3 day reperfusion and may

contribute to sustained translation arrest and CA1 pyramidal neuron vulnerability (DeGracia et al. 2007). In addition, in primary mouse astrocyte cultures subject to glucose deprivation, the ubiquitin-immunolabeling shows heterogeneous, clumped protein aggregates (Qiao et al. 2003). Protein aggregation with reduced cytosolic and nucleus free ubiquitin distribution has also been detected in organotypic hippocampal slice culture model of cerebral ischemia (Ouyang et al. 2005).

In the current study, we detected a time-dependent accumulation of ubiquitin-conjugated protein aggregates following 2 h OGD and 2–24 h REOX in pure neuronal cultures. Following OGD, neurons exhibited loss of free ubiquitin staining, formation of smear TX-insoluble ubi-proteins, and deposition of ubiquitin clusters in peri-nucleus regions. This study provides first line evidence that protein aggregate formation occurs in disassociated neuronal cultures under OGD conditions. Interestingly, the temporal profile of these changes is similar to those in ischemic brain tissues (Hu et al. 2000).

Role of NKCC1/NCX_{rev} in altered protein aggregation and degradation following OGD/REOX

The molecular mechanisms underlying the formation of protein aggregates are not well understood. Accumulation of ubiquitinated proteins is in part an imbalance between formation of misfolded proteins in ER and proteasomal function. ER expresses abundant chaperones and protein folding enzymes which regulate appropriate folding of a large variety of proteins and prevent protein aggregation (Corbett and Michalak 2000). Ischemic-induced ATP depletion has been suggested to damage protein folding processes and protein folding machinery such as molecular chaperones (Liu et al. 2005). Indeed, in this study, we found a strong negative correlation ($r^2 = 0.82$) between protein aggregate formation and ATP levels following OGD/REOX (data not shown). Without functional molecular chaperones, newly synthesized proteins cannot fold, and will form ubiquitinated misfolded proteins (Groenendyk and Michalak 2005). Interchaperone interactions and folding of newly synthesized glycoproteins also depend on appropriate levels of ER Ca^{2+} (Meldolesi and Pozzan 1998). Thus, depletion of $Ca^{2+}{}_{ER}$ could be the initial signal leading to ER dysfunction and accumulation of unfolded proteins in post-OGD neurons.

We recently demonstrated that depletion of $Ca^{2+}{}_{ER}$ occurs in neurons at 15 min REOX after 2 h OGD (Chen et al. 2008). NKCC1 and NCX_{rev} contribute to the initial overload of $Ca^{2+}{}_{ER}$ during OGD and subsequent $Ca^{2+}{}_{ER}$ release during REOX (Chen et al. 2008). Reducing $Ca^{2+}{}_{ER}$ dysregulation by blocking NKCC1/NCX_{rev} significantly attenuates expression of ER stress proteins and cell death (Chen et al. 2008). Interestingly, in the current study, we found that inhibition of NKCC1 activity decreased formation of ubiquitin-conjugated protein aggregates during 2–24 h REOX. Moreover, inhibition of NKCC1 (pharmacologically or genetically) significantly attenuated formation of ubiquitin clusters in peri-nucleus regions and loss of free ubiquitin. These data clearly demonstrate that blocking NKCC1 activity reduces accumulation of protein aggregates. We believe that this protection, in part, results from reducing NKCC1/NCX_{rev}-mediated ER Ca^{2+} dysregulation (Figure 5). This hypothesis is further supported by the finding that thapsigargin promoted protein aggregate formation, whereas the NCX_{rev} inhibitor SEA0400 reduced OGD/REOX-mediated aggregate formation.

Changes of proteasomal activity following OGD/REOX

ER malfolded proteins can trigger their transport out of ER lumen and the ubiquitination and proteasome-mediated degradation (ER associated protein degradation) (Brodsky 2007). Proteasomes are non-lysosomal, multicatalytic proteinase complexes involved in the degradation of most intracellular short-lived proteins (Hershko and Ciechanover 1998). A time-dependent decrease in proteasome activity has been detected in ipsilateral cortex and hippocampus during 1– 24 h reperfusion after transient focal ischemia (Keller et al. 2000). The

authors attribute the ischemia-induced proteasome inhibition in part to oxidative stress (Keller et al. 2000). In the current study, we observed that the proteasome activity was inhibited by 80–90% during 2–8 h REOX and recovered partially at 24 h REOX. Interestingly, pharmacological inhibition or genetic ablation of NKCC1 activity completely rescued proteasome activity inhibition at 2 h REOX, which was accompanied with higher ATP content preservation. However, at later time points, Bu treatment provided significant but incomplete protection against OGD/REOX-mediated loss of proteasome activity. This suggests that inhibition of proteasome activity under these conditions only partially involves NKCC1 activity. We also observed a general trend for proteasome activity during REOX to be accompanied with higher ATP content preservation (r^2= 0.51, data not shown). Notably, intracellular ATP level and proteasome activity remained nearly normal in NKCC1$^{-/-}$ neurons after 2 h OGD/24 h REOX. A characteristic feature of proteasomal protein degradation is the linkage between proteolysis and ATP hydrolysis (300–400 ATP molecules/molecule of protein substrate) which is needed for substrate unfolding, gate opening, and substrate translocation (Benaroudj et al. 2003). Our results suggest that inhibition of NKCC1 activity may reduce protein aggregates in part via preserving intracellular ATP levels and proteasome function.

Our $[Na^+]_i$ determination showed that inhibition of NKCC1-mediated Na^+ entry significantly attenuates intracellular Na^+ accumulation following OGD/REOX. These findings suggest that Na^+/K^+-ATPase function is not sufficient to maintain Na^+_i homeostasis following OGD/REOX. Inhibition of NKCC1 during REOX only partially inhibited Na^+ accumulation, suggesting a role for other routes of Na^+ entry, such as ionotropic glutamate receptors or TTX-sensitive channels (Muller and Somjen 2000).

Previously, we have established that ouabain-dependent Na^+ accumulation during 0–15 min REOX in neurons is not significantly different from normoxia (Chen et al. 2008). This suggests that following OGD Na^+ accumulation in cultured neurons is the result of increases in Na^+ influx that outstrips Na^+/K^+-ATPase function. Thus, blocking NKCC1 activity could preserve intracellular ATP content in part by reducing NKCC1-mediated Na^+ entry, which would decrease the need for Na^+ extrusion via Na^+/K^+-ATPase. This is consistent with the report that hypoxia-induced ATP reduction and damage in hippocampal CA1 neurons are attenuated by the Na^+ channel inhibitors (Raley-Susman et al. 2001). The NKCC1 inhibitor bumetanide restores ATP levels in neurons in ischemic hippocampal slices (Pond et al. 2004). However, it is also clear that NKCC1 activity is not the sole contributor to ATP preservation following OGD/REOX.

It should be noted that irreversible ATP-independent inhibition of proteasome activity has been detected in ischemic CA1 neurons after transient forebrain ischemia (Asai et al. 2002). In our study, both proteasome activity and ATP levels tended to recover during 0–24 h REOX. There was one exception, in the presence of Bu, where neurons exhibited a complete recovery of proteasomal activity despite only partial recovery of intracellular ATP after 2 h OGD/2 h REOX. This suggests that biphasic mechanisms may be involved in regulation of proteasome activity after OGD/REOX. Several studies have shown that proteasomes could be impaired via oxidative stress after cerebral ischemia-reperfusion. Mice overexpressing the antioxidant enzyme glutathione peroxidase display reduced levels of proteasome inhibition (Keller et al. 2000). Irreversible inhibition of proteasome activity has been detected in ischemic CA1 neurons after transient forebrain ischemia in an ATP-regenerating system (Asai et al. 2002), suggesting ATP-independent inhibition of proteasome. Thus, these mechanisms may play a role in irreversible inhibition of proteasome activity. However, in the current study, depression of proteasome activity and persistent protein aggregation were reversed with recovery of intracellular ATP at 24 h post-OGD. This is in contrast to the characteristic dissociation between these processes in *in vivo* transient cerebral ischemia (Hermann et al. 2001; DeGracia

and Hu 2007). These findings reflect the limitation of the OGD model in studying the latter phenomena.

Taken together, in this study, we demonstrate for the first time that OGD treatment led to a time-dependent formation of ubiquitin-conjugated protein aggregates in disassociated neuronal cultures. Aggregate formation resulted from increases in misfolded protein production and inhibition of ATP-dependent proteasome activity. Interestingly, blocking NKCC1 and NCX_{rev} significantly reduced formation of insoluble protein aggregates and better preserved intracellular ATP and Na^+_i homeostasis. Our findings suggest that dysregulation of Na^+ and Ca^{2+} ionic homeostasis via activation of NKCC1 and NCX_{rev} contributes to protein folding and degradation following ischemia.

Acknowledgments

This work was supported in part by NIH grants R01NS38118 and R01NS048216 (D. Sun), and an AHA Established-Investigator award grant N0540154 (D. Sun).

Abbreviations

BCA	bicinchoninic acid
Bu	bumetanide
Ca^{2+}_{ER}	endoplasmic reticulum Ca^{2+}
DIV	days *in vitro*
DTT	dithiothreitol
ER	endoplasmic reticulum
IP_3R	inositol 1,4,5-trisphosphate receptor
NCX	Na^+/Ca^{2+} exchanger
NCX_{rev}	reversed mode operation of NCX
NKCC1	Na^+-K^+-Cl^- cotransporter isoform 1
OGD	oxygen and glucose deprivation
REOX	reoxygenation
RyR	ryanodine receptor
SBFI	sodium-binding benzofuran isophthalate
SERCA	sarco/endoplasmic reticulum Ca^{2+}-ATPase
ubi-proteins	ubiquitin-conjugated proteins
$[Na^+]_i$	intracellular Na^+ concentration

Reference List

Asai A, Tanahashi N, Qiu JH, Saito N, Chi S, Kawahara N, Tanaka K, Kirino T. Selective proteasomal dysfunction in the hippocampal CA1 region after transient forebrain ischemia. J Cereb Blood Flow Metab 2002;22:705–710. [PubMed: 12045669]

Beck J, Lenart B, Kintner DB, Sun D. Na-K-Cl cotransporter contributes to glutamate-mediated excitotoxicity. J Neurosci 2003;23:5061–5068. [PubMed: 12832529]

Benaroudj N, Zwickl P, Seemuller E, Baumeister W, Goldberg AL. ATP hydrolysis by the proteasome regulatory complex PAN serves multiple functions in protein degradation. Mol Cell 2003;11:69–78. [PubMed: 12535522]

Brodsky JL. The protective and destructive roles played by molecular chaperones during ERAD (endoplasmic-reticulum-associated degradation). Biochem J 2007;404:353–363. [PubMed: 17521290]

Chen X, Kintner DB, Luo J, Baba A, Matsuda T, Sun D. Endoplasmic reticulum Ca(2+) dysregulation and endoplasmic reticulum stress following in vitro neuronal ischemia: role of Na(+)-K(+)-Cl(−) cotransporter. J Neurochem 2008;106:1563–1576. [PubMed: 18507737]

Corbett EF, Michalak M. Calcium, a signaling molecule in the endoplasmic reticulum? Trends Biochem Sci 2000;25:307–311. [PubMed: 10871879]

DeGracia DJ, Hu BR. Irreversible translation arrest in the reperfused brain. J Cereb Blood Flow Metab 2007;27:875–893. [PubMed: 16926841]

DeGracia DJ, Rudolph J, Roberts GG, Rafols JA, Wang J. Convergence of stress granules and protein aggregates in hippocampal cornu ammonis 1 at later reperfusion following global brain ischemia. Neuroscience 2007;146:562–572. [PubMed: 17346899]

Eytan E, Ganoth D, Armon T, Hershko A. ATP-dependent incorporation of 20S protease into the 26S complex that degrades proteins conjugated to ubiquitin. Proc Natl Acad Sci U S A 1989;86:7751–7755. [PubMed: 2554287]

Flagella M, Clarke LL, Miller ML, Erway LC, Giannella RA, Andringa A, Gawenis LR, Kramer J, Duffy JJ, Doetschman T, Lorenz JN, Yamoah EN, Cardell EL, Shull GE. Mice lacking the basolateral Na-K-2Cl cotransporter have impaired epithelial chloride secretion and are profoundly deaf. J Biol Chem 1999;274:26946–26955. [PubMed: 10480906]

Ge P, Luo Y, Liu CL, Hu B. Protein aggregation and proteasome dysfunction after brain ischemia. Stroke 2007;38:3230–3236. [PubMed: 17975104]

Groenendyk J, Michalak M. Endoplasmic reticulum quality control and apoptosis. Acta Biochim Pol 2005;52:381–395. [PubMed: 15933766]

Haas AL, Rose IA. The mechanism of ubiquitin activating enzyme. A kinetic and equilibrium analysis. J Biol Chem 1982;257:10329–10337. [PubMed: 6286650]

Hermann DM, Kilic E, Hata R, Hossmann KA, Mies G. Relationship between metabolic dysfunctions, gene responses and delayed cell death after mild focal cerebral ischemia in mice. Neuroscience 2001;104:947–955. [PubMed: 11457582]

Hershko A, Ciechanover A. The ubiquitin system. Annu Rev Biochem 1998;67:425–479. [PubMed: 9759494]

Hu BR, Janelidze S, Ginsberg MD, Busto R, Perez-Pinzon M, Sick TJ, Siesjo BK, Liu CL. Protein aggregation after focal brain ischemia and reperfusion. J Cereb Blood Flow Metab 2001;21:865–875. [PubMed: 11435799]

Hu BR, Martone ME, Jones YZ, Liu CL. Protein aggregation after transient cerebral ischemia. J Neurosci 2000;20:3191–3199. [PubMed: 10777783]

Ide T, Takada K, Qiu JH, Saito N, Kawahara N, Asai A, Kirino T. Ubiquitin stress response in postischemic hippocampal neurons under nontolerant and tolerant conditions. J Cereb Blood Flow Metab 1999;19:750–756. [PubMed: 10413029]

Kakizuka A. Protein precipitation: a common etiology in neurodegenerative disorders? Trends Genet 1998;14:396–402. [PubMed: 9820028]

Keller JN, Huang FF, Zhu H, Yu J, Ho YS, Kindy TS. Oxidative stress-associated impairment of proteasome activity during ischemia-reperfusion injury. J Cereb Blood Flow Metab 2000;20:1467–1473. [PubMed: 11043909]

Lenart B, Kintner DB, Shull GE, Sun D. Na-K-Cl cotransporter-mediated intracellular Na^+ accumulation affects Ca^{2+} signaling in astrocytes in an in vitro ischemic model. J Neurosci 2004;24:9585–9597. [PubMed: 15509746]

Liu CL, Ge P, Zhang F, Hu BR. Co-translational protein aggregation after transient cerebral ischemia. Neuroscience 2005;134:1273–1284. [PubMed: 16039801]

Meldolesi J, Pozzan T. The endoplasmic reticulum Ca^{2+} store: a view from the lumen. Trends Biochem Sci 1998;23:10–14. [PubMed: 9478128]

Muller M, Somjen GG. Na(+) dependence and the role of glutamate receptors and Na(+) channels in ion fluxes during hypoxia of rat hippocampal slices. J Neurophysiol 2000;84:1869–1880. [PubMed: 11024079]

Ouyang YB, Xu L, Giffard RG. Geldanamycin treatment reduces delayed CA1 damage in mouse hippocampal organotypic cultures subjected to oxygen glucose deprivation. Neurosci Lett 2005;380:229–233. [PubMed: 15862891]

Paschen W, Doutheil J. Disturbances of the functioning of endoplasmic reticulum: a key mechanism underlying neuronal cell injury? J Cereb Blood Flow Metab 1999;19:1–18. [PubMed: 9886350]

Pond BB, Galeffi F, Ahrens R, Schwartz-Bloom RD. Chloride transport inhibitors influence recovery from oxygen-glucose deprivation-induced cellular injury in adult hippocampus. Neuropharmacology 2004;47:253–262. [PubMed: 15223304]

Qiao Y, Ouyang YB, Giffard RG. Overexpression of HDJ-2 protects astrocytes from ischemia-like injury and reduces redistribution of ubiquitin staining in vitro. J Cereb Blood Flow Metab 2003;23:1113–1116. [PubMed: 14526221]

Raley-Susman KM, Kass IS, Cottrell JE, Newman RB, Chambers G, Wang J. Sodium influx blockade and hypoxic damage to CA1 pyramidal neurons in rat hippocampal slices. J Neurophysiol 2001;86:2715–2726. [PubMed: 11731531]

Russell JM. Sodium-potassium-chloride cotransport. Physiol Rev 2000;80:211–276. [PubMed: 10617769]

Zhang F, Liu CL, Hu BR. Irreversible aggregation of protein synthesis machinery after focal brain ischemia. J Neurochem 2006;98:102–112. [PubMed: 16805800]

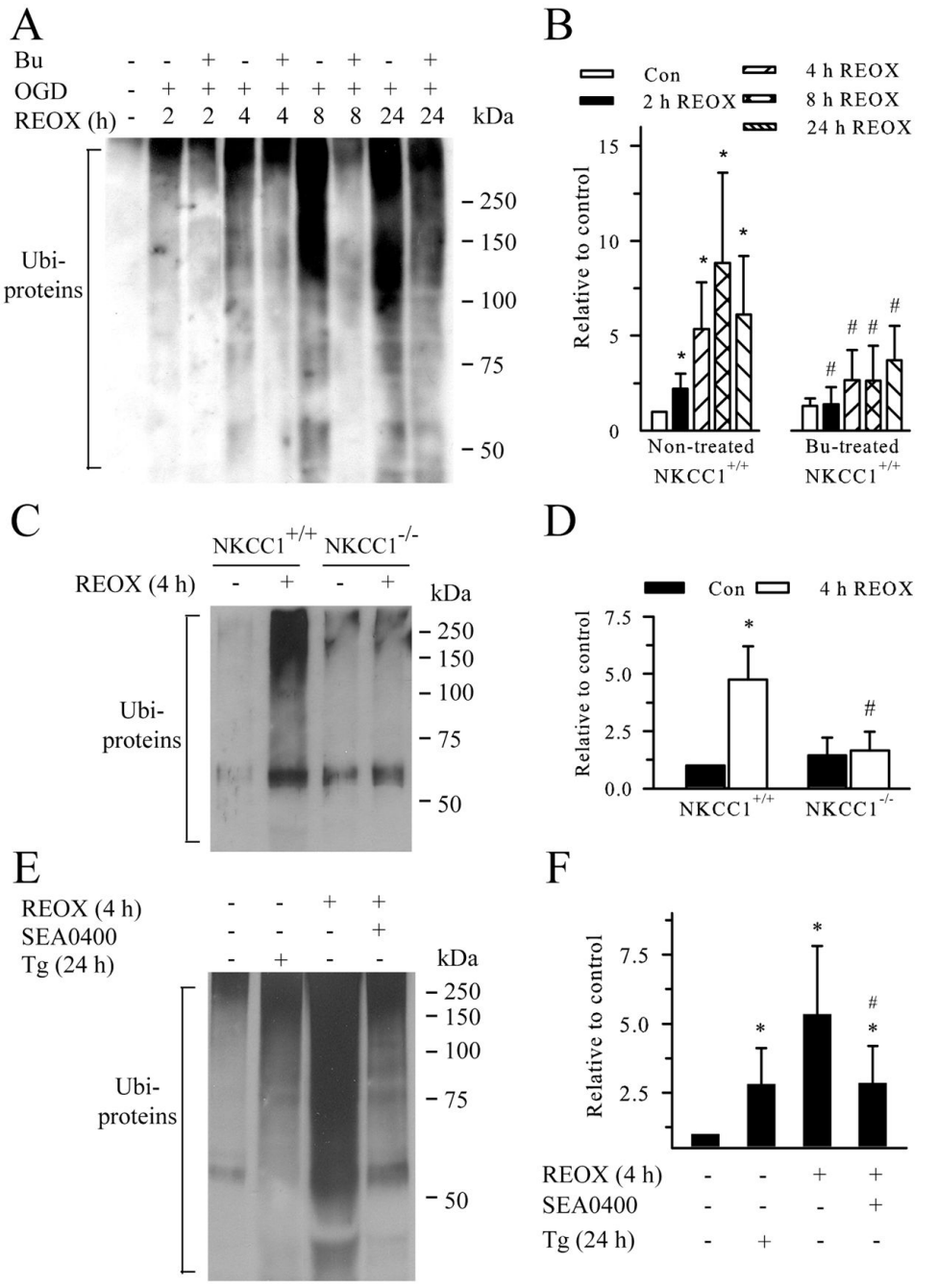

Figure 1. Inhibition of NKCC1/NCX$_{rev}$ attenuates protein aggregate formation following OGD/REOX

A. Inhibition of NKCC1 activity by bumetanide attenuated formation of ubi-protein aggregates. TX-100-insoluble protein fractions were obtained from cellular lysates (500 μg protein) of normoxic controls and OGD/REOX-treated cultures. Protein smear ranged between 37–250 kDa in each lane as detected by a monoclonal anti-ubiquitin antibody. In the case of Bu treatment, 10 μM Bu was added 30 min prior to OGD and present in all subsequent incubations. **B.** Summary data. Ubi-proteins were quantified using average intensity of protein smear in each lane with ImageJ software and data were presented as relative change to control. Data are mean ± SD. n = 3–7. * $p < 0.05$ vs. normoxic control; # $p < 0.05$ vs. non-treated. **C.** Effects of

NKCC1 gene ablation on formation of ubi-proteins. $NKCC1^{-/-}$ and $NKCC1^{+/+}$ cultures from the same littermates were subjected to 2 h OGD and 4 h REOX in parallel. **D.** Summary data. Data are mean ± SD. n = 4. * $p < 0.05$ vs. $NKCC1^{+/+}$ normoxic control; # $p < 0.05$ vs. $NKCC1^{+/+}$ 4 h REOX. **E.** Effects of inhibition of NCX_{rev} activity or SERCA on formation of ubi-proteins. NCX_{rev} inhibitor SEA0400 (1 μM) was present at 0–4 h REOX or 0.1 μM Tg was present for 24 h. **F.** Summary data. Data are mean ± SD. n = 3–4. * $p < 0.05$ vs. normoxic control; # $p < 0.05$ vs. 4 h REOX. Statistical significance was determined by paired student's *t* test between the two groups.

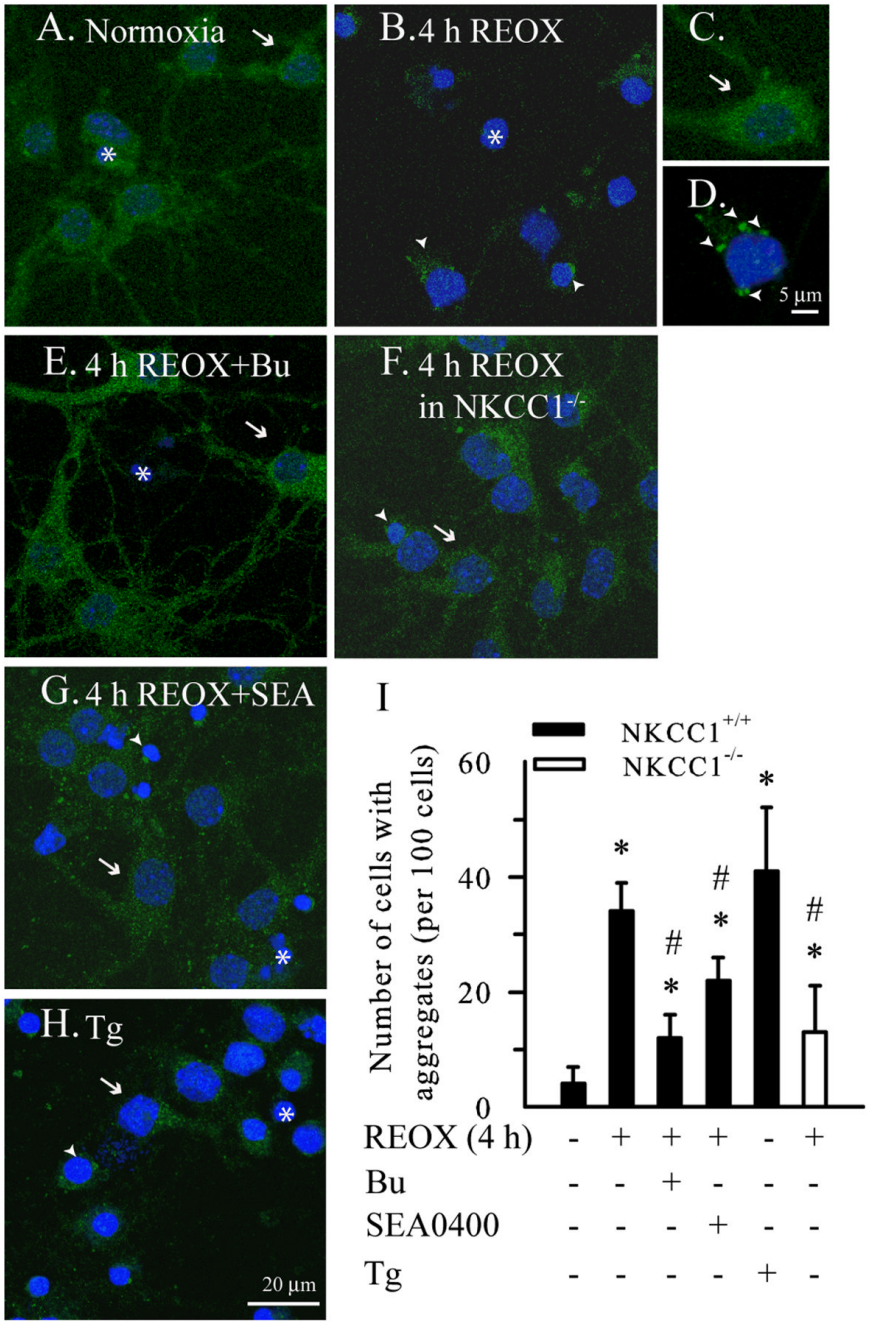

Figure 2. Detection of ubiquitin-conjugated proteins with immunostaining

Ubiquitin distribution was analyzed with the anti-ubiquitin monoclonal antibody using confocal microscopy. Drug treatments were identical to Figure 1. **A.** Normoxic control. **B.** 2 h OGD/4 h REOX. **C, D**. Magnified images of neurons in **A** and **B. E.** 2 h OGD/4 h REOX plus Bu. **F.** NKCC1$^{-/-}$ neurons following 2 h OGD/4 h REOX. **G.** 2 h OGD/4 h REOX plus SEA0400. **H.** Tg for 24 h. **I.** Summary data. Data are mean ± SD. n = 3–5. * $p < 0.05$ vs. normoxic control; $^{\#}$ $p < 0.05$ vs. 4 h REOX. Green: ubiquitin immunosignals. Blue: nucleus staining with To-pro-3 iodide. **Arrow**: cell with normal ubiquitin distribution. **Arrowhead**: cell with ubi-proteins. **Asterisk**: nuclei.

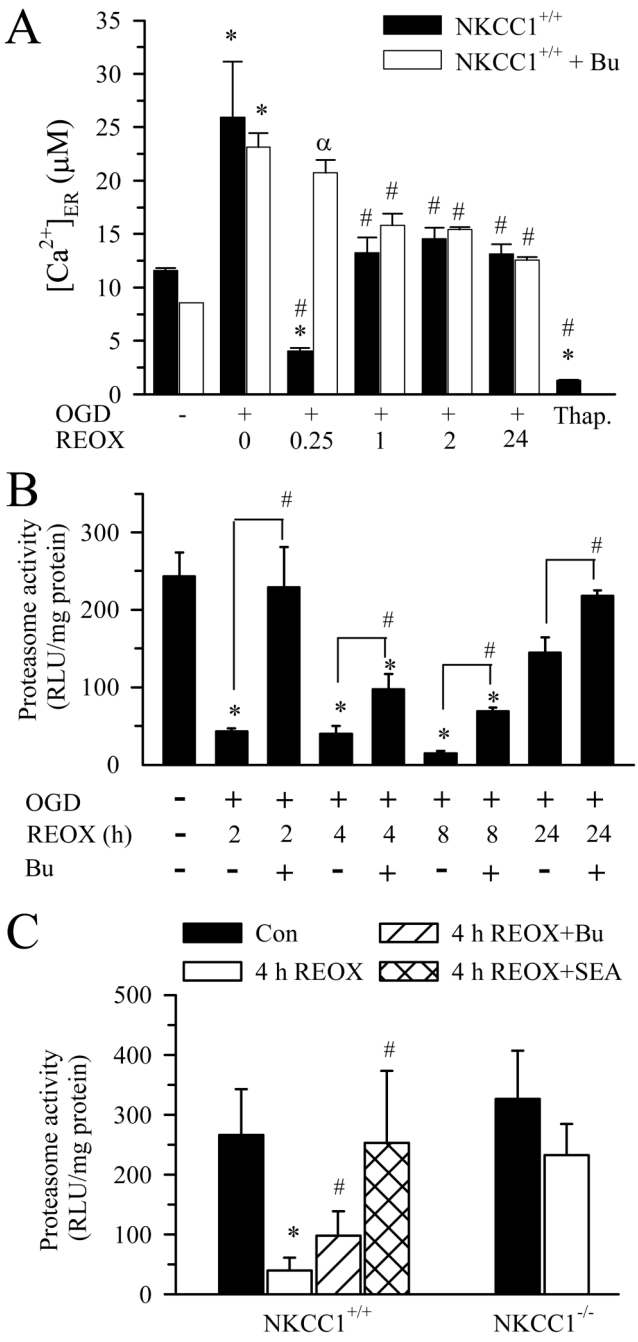

Figure 3. Changes of ER Ca^{2+} and proteasomal activity following OGD/REOX

A. ER Ca^{2+} was determined in neurons subjected to 2 h OGD and 0–24 h REOX. In the bumetanide studies, neurons were pretreated with 10μM bumetanide that was then present throughout the experiment. In some experiments, neurons were subjected to 0.1 μM Tg for 24 h. Data are mean ± SEM. n = 3–9. * $p < 0.05$ vs. normoxic control; # $p < 0.05$ vs. corresponding 0 REOX; α $p < 0.05$ vs corresponding non-treated. **B.** Proteasomal activity in neurons under different conditions. $NKCC1^{+/+}$ neurons were subjected to 2 h OGD and 2, 4, 8, 24 h REOX. In the case of Bu treatment, 10 μM Bu was added 30 min prior to OGD and present in all subsequent incubations. Data are means ± SEM. n = 3–4. * $p < 0.05$ vs. normoxic control; # $p < 0.05$ vs. corresponding non-treated. **C.** Effects of inhibition of NCX_{rev} and NKCC1 activity

on proteasomal activity. $NKCC1^{-/-}$ and $NKCC1^{+/+}$ littermate cultures were subjected to 2 h OGD and 4 h REOX. In SEA0400 treatment, 1 μM SEA0400 was present at 0–4 h REOX. In the case of Bu treatment, 10 μM Bu was added 30 min prior to OGD and present in all subsequent incubations. Data are mean ± SEM. n = 4. * $p < 0.05$ vs. $NKCC1^{+/+}$ normoxic control; # $p < 0.05$ vs. $NKCC1^{+/+}$ 4 h REOX.

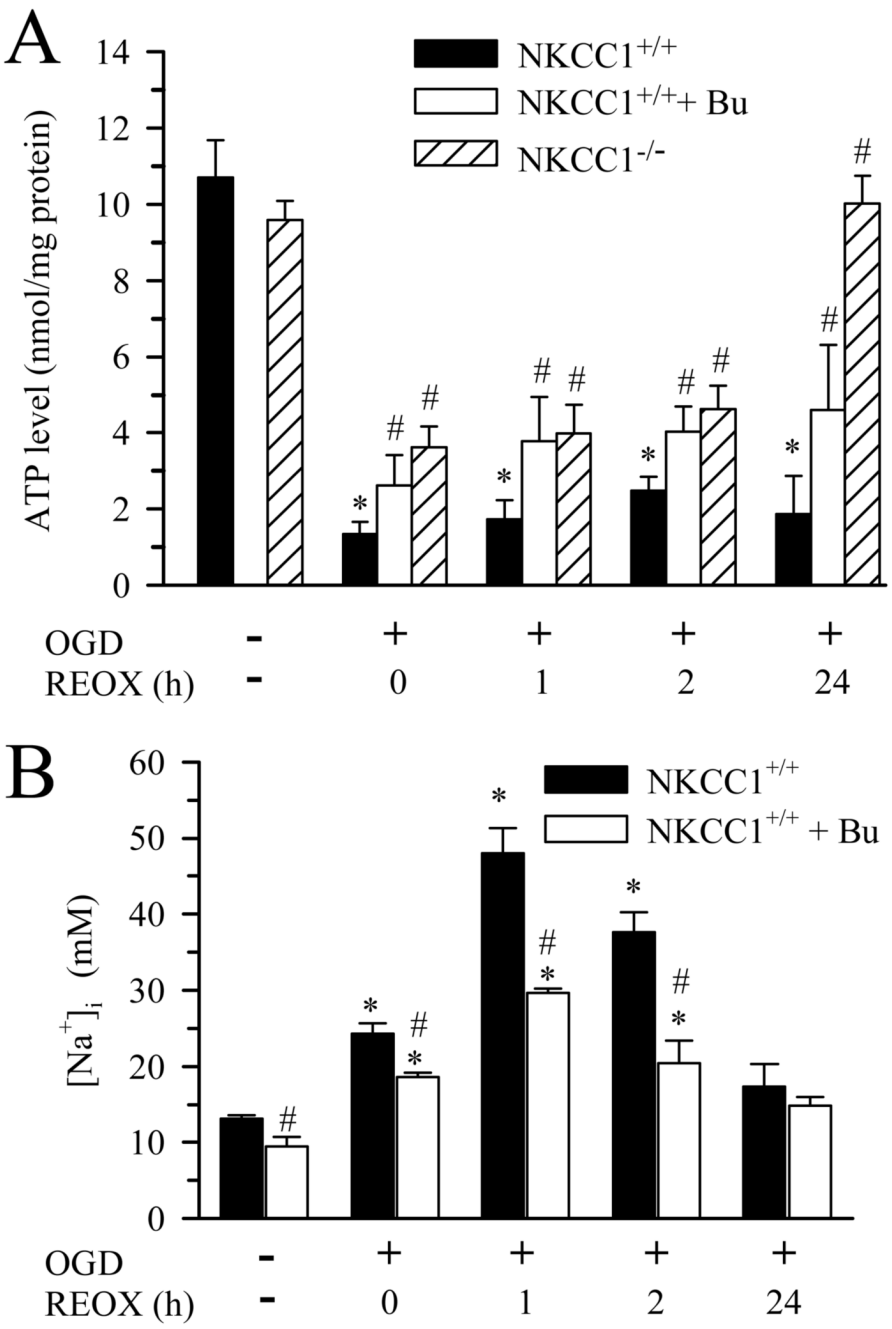

Figure 4. Changes of intracellular ATP and $[Na^+]_i$ following OGD/REOX

A. Intracellular ATP content in neurons subjected to 2 h OGD and 0, 1, 2, or 24 h REOX was determined using a luminescence ATP detection assay. Data are mean ± SEM. n = 3–9. * $p < 0.05$ vs. normoxic control; # $p < 0.05$ vs. corresponding non-treated REOX. **B.** $[Na^+]_i$ was determined in neurons subjected to 2 h OGD and 0–24 h REOX. 10μM Bu was used as described in Figure 3. Data are mean ± SEM. n = 3–4 * $p < 0.05$ vs. corresponding normoxic control; # $p < 0.05$ vs. corresponding non-treated.

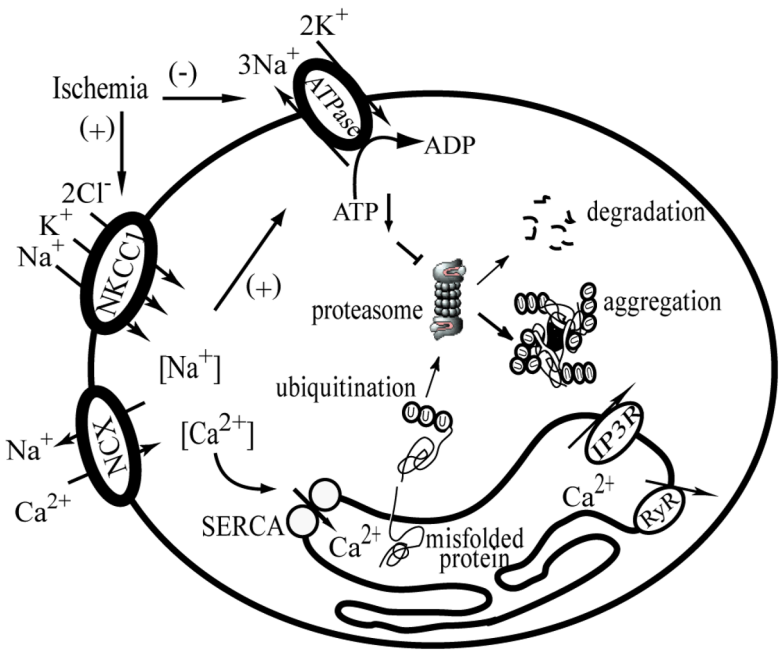

Figure 5. Illustration of Na^+ and Ca^{2+} disruption and protein aggregate formation in ischemic neurons

Following ischemia, activation of NKCC1 causes an increase in $[Na^+]_i$ which triggers NCX_{rev} and leads to increases in $[Ca^{2+}]_i$. The $[Na^+]_i$ overload also causes increased consumption of ATP by the Na^+/K^+-ATPase to maintain ionic homeostasis which may subsequently affect ATP-dependent proteasome activity. On the other hand, the $[Ca^{2+}]_i$ overload results in an initial Ca^{2+}_{ER} overload by SERCA and subsequent Ca^{2+}_{ER} release following activation of inositol 1,4,5-trisphosphate receptor (IP_3R) and ryanodine receptor (RyR). The depletion of Ca^{2+}_{ER} may cause accumulation of misfolded proteins and protein aggregates. Blocking NKCC1 and NCX_{rev} would reduce disruption of Na^+ and Ca^{2+} homeostasis and improve ATP-dependent proteasome activity.